Simulation of an Industrial Fluid Catalytic Cracking Riser Reactor Using a Novel 10-Lump Kinetic Model and Some Parametric Sensitivity Studies

Article *in* Industrial & Engineering Chemistry Research · December 2014

DOI: 10.1021/ie5006433

CITATIONS
8

READS
56

6 authors, including:

Prabha K Dasila
Bharat Petroleum
4 PUBLICATIONS **32** CITATIONS

SEE PROFILE

Sawaran Jit Chopra
University of Petroleum & Energy Studies
5 PUBLICATIONS **37** CITATIONS

SEE PROFILE

I&EC research
Industrial & Engineering Chemistry Research

Article

pubs.acs.org/IECR

Simulation of an Industrial Fluid Catalytic Cracking Riser Reactor Using a Novel 10-Lump Kinetic Model and Some Parametric Sensitivity Studies

Prabha K. Dasila,*[,†,‡] Indranil R. Choudhury,[‡] Sanjeev Singh,[‡] Santanam Rajagopal,[‡] Sawaran J. Chopra,[†] and Deoki N. Saraf[†]

[†]University of Petroleum & Energy Studies, Dehradun 248007, India

[‡]Research & Development Centre, Indian Oil Corporation Ltd., Faridabad 121007, India

ABSTRACT: A fluid catalytic cracking (FCC) unit has been simulated by integrating FCC riser reactor and regenerator models. This simulation uses a new10-lump riser reactor kinetic model developed in-house. The lumping scheme and reactions are based on more detailed description of the feed in terms of PNA (paraffins, naphthenes, and aromatics) in both light and heavy fractions. An artificial neural network (ANN) model, also developed in-house, relates routinely measured properties such as specific gravity, ASTM temperatures, and so on to the detailed feed composition needed for the kinetic model development. The conversion and product yields obtained by integrating the model equations were found to be in close agreement with those measured in the plant in all the cases investigated. Simulation results using the present model, when compared with results from a conventional 5-lump model, clearly brought out the improvement in prediction because of detailed feed description calculated from ANN models. A parametric sensitivity study was undertaken with respect to operating conditions such as effects of feed preheat temperature, feed flow rate, and reactor outlet temperature (independent variables) on the performance of the FCC unit, and the results have been discussed.

1. INTRODUCTION

Fluid catalytic cracking (FCC) is an important secondary process, converting low-priced heavy feed stocks such as heavy oil from either the refinery crude unit or vacuum unit and heavy fractions from other conversion units (cooker gas oil, hydrocracker fractionator bottoms, and so on) into lighter, more valuable hydrocarbons such as liquefied petroleum gas (LPG) and gasoline, thus increasing the profitability of the entire refinery. Coke is formed as a byproduct during the process along with dry gas, both of which are undesirable. The conversion and yield pattern strongly depend on the feedstock quality, operating conditions of the riser reactor−regenerator sections and the type of catalyst.

The FCC process is very complex due to complicated hydrodynamics, heat transfer and mass transfer effects, and complex cracking kinetics. These complex interactions coupled with the economic importance of the unit have prompted many researchers to put their efforts into the modeling of FCC processes. Additionally, a small improvement in the operation or control of an FCC unit (FCCU) can result in impressive economic benefits. However, these can be achieved only if a satisfactory mathematical model is available which is analytical so that its optimization can lead to optimal operating conditions. Modeling is an iterative process and leads to deeper understanding of the physics involved, which can be used for designing better control of the process unit. Process optimization can lead to improved productivity by maximizing throughput and choosing optimal operating conditions. Online optimization can help maximize long-term profits by reducing the cost and improving yields. Additionally, running a model simultaneously in parallel with the plant operation can help in monitoring the plant and its health.

There are several modeling approaches for FCCUs available in the literature.[1−14] The kinetic lumping approach has been most widely used in which the large number of feed and the product hydrocarbons are lumped into a few groups, called kinetic lumps, which are assumed to take part in the reactions as single entities. A number of kinetic models have been developed by various researchers using 2, 3, 4, 5, 6, 8, 10, or 12 lumps, but because of the complexities involved, a completely satisfactory model has eluded each one so far. The FCC kinetic modeling is based on a specified number of lumps for feedstock and products rather than on individual molecules. These lumps are considered either on the basis of the boiling range of the feedstock and corresponding products in the reaction system or on the basis of the type of hydrocarbon groups.[10] Each type of hydrocarbon is assumed as one lump, and the products are considered by different lumps according to their boiling range. In the often used, feed specific 5-lump model, the feed is represented by a single lump of average carbon number and molecular weight and gasoline, LPG, dry gas, and coke, present in the product stream, along with unconverted feed are the remaining lumps.[5−9] The limitation of models using a single lump feed description is that the kinetics is valid only for the particular vacuum gas oil (VGO) with which the model parameters were estimated and is generally not applicable to other feeds especially

Special Issue: Energy System Modeling and Optimization Conference 2013

Received: February 15, 2014
Revised: July 27, 2014
Accepted: August 24, 2014

   dx.doi.org/10.1021/ie5006433 | *Ind. Eng. Chem. Res.* XXXX, XXX, XXX−XXX

if the composition is significantly different. The available 10- and 12-lump models are more accurate where the feed is described in terms of 6 or 8 kinetic lumps consisting of the heavy and light fractions of paraffins, naphthenes, and aromatics (PNA),[10−15] but these detailed kinetic models suffer from the requirement of detailed feed composition analysis which is seldom possible in a field laboratory.

In the present work, a simulator embedding a 10-lump kinetic model of the riser reactor developed in our earlier work[15] was integrated with a regenerator model to simulate the FCC process. The product yields were obtained by integrating the model equations along the length of the reactor. The detailed feed composition in terms of heavier and lighter fractions of P, N, and A required as input to the kinetic model was obtained from a validated artificial neural network (ANN) model.[16] The neural network model used routinely measured feed properties in field laboratories such as specific gravity, ASTM temperatures, and so on as input.

Parametric sensitivity studies can provide valuable information to the plant operator where the operator learns the effect of variations in the independent operating variables on the plant performance. The effects of variation in three independent variables, feed flow rate, feed temperature, and reactor outlet temperature, on conversion and product yields have been investigated. Finally a comparison has been made between the performances of the simulator with 10-lump and 5-lump kinetics.

2. DESCRIPTION OF FLUID CATALYTIC CRACKING PROCESS

FCC units operate at high temperature and moderate pressure with finely divided silica-/alumina-based catalyst. One of the important advantages of FCC is the ability of the catalyst to flow easily when fluidized with reaction mixture in the vapor phase. Due to this fluidization of the catalyst, there is intimate interaction between the catalyst and hydrocarbons leading to more cracking reactions.

The main components of an FCCU are riser reactor and regenerator as shown in Figure 1. A partially vaporized heavy

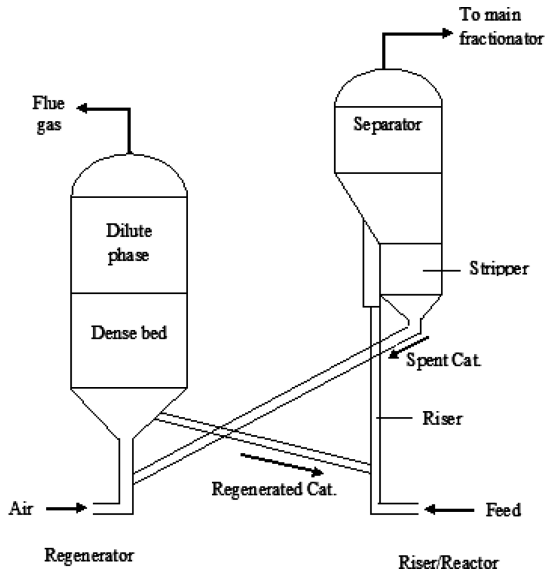

Figure 1. Schematic diagram of the fluid catalytic cracking unit.

gas oil/vacuum gas oil charge meets a stream of regenerated hot catalyst at the base of the riser. The liquid droplets of the feed receive heat from the hot catalyst particles and almost instantaneously vaporize. As the vapors and catalyst particles move up the riser, the cracking reactions take place. Carbon generated during cracking reactions gets deposited on the catalyst surface and cracking activity progressively decreases. At the exit of the reactor, catalyst is separated from the reaction mass, adsorbed hydrocarbons are stripped off in a stripper with the help of steam, and the spent catalyst is sent to the regenerator. In the regenerator, the catalyst is continuously regenerated by burning off the coke deposited during the cracking reaction. Other auxiliary units such as feed preheat, air, and flue gas systems are required for operation of the unit but have not been included in the modeling exercise

3. MODELING OF FLUID CATALYTIC CRACKING UNIT

In the present work, a 10-lump kinetic model, developed in-house, was integrated with a regenerator model for the simulation of the entire FCC unit. The steam stripper was assumed to be ideal, and hence its modeling was not included.

3.1. Riser/Reactor Model. A 10-lump kinetic description for the riser reactor reported in our previous work[15] has been used for the present study. A total of 25 cracking reactions have been accounted for, and the reaction scheme is shown in Figure 2.

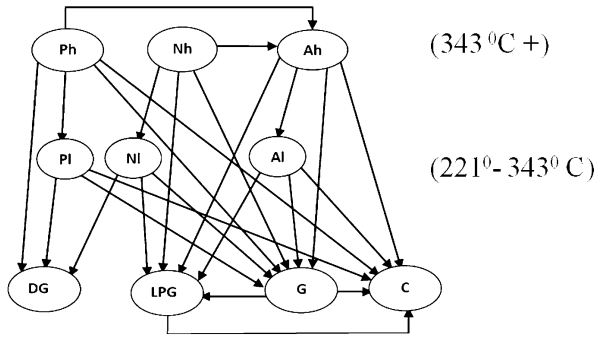

Figure 2. Ten-lump kinetic scheme.

The detailed lumping scheme uses 6 lumps to describe the feed gas oil, namely, heavy paraffins, heavy naphthenes, heavy aromatics, light paraffins, light naphthenes, and light aromatics. This means we need the compositions in terms of these lumps for every new feed used. To circumvent the problem of having to measure detailed composition which is not very practical in field laboratories, an ANN-based model was developed which provided the requisite composition as output, input being routinely measured properties of VGO such as specific gravity, ASTM distillation temperatures, Conradson carbon residue (CCR), total sulfur, and total nitrogen.[16] The detailed PNA analysis of several VGO samples for ANN model development were measured in the laboratory by using high-resolution mass spectrometric method.[16]

The complete set of model equations for the riser reactor and stripper are given in Appendix A. The following assumptions from literature[10−14] were made to develop the kinetic model of the riser reactor: All cracking reactions are first order; the reaction mass consists of only two phases (solid and vapor phases); heat capacities and densities are constant throughout the length of the reactor; catalyst deactivation is nonselective and related to the coke on the catalyst[17,18] only; the solid catalyst particles are in thermal equilibrium with the gaseous mixture at all times; the flow is uniform, that is, there is no slip between solid catalyst and vapors; LPG and gasoline do not crack to produce dry gas, and dry gas produces no coke.

dx.doi.org/10.1021/ie5006433 | Ind. Eng. Chem. Res. XXXX, XXX, XXX−XXX

The aim of the stripper is to remove residual hydrocarbons from the catalyst surface after cracking reactions. Being a minor unit, no effort was made to rigorously model this unit. The spent catalyst temperature and flow rate were calculated from the model equations available in Appendix A. A temperature drop of 10 K was assumed across the stripper unit.[5,8]

3.2. Regenerator Model. An FCC regenerator usually consists of a large fluidized bed reactor with coke combustion kinetics and complex hydrodynamics. The deposited coke on the catalyst surface during the cracking reactions in the riser is burned off in the regenerator in the presence of air. These coke combustion reactions taking place in the regenerator are strongly exothermic. There are usually two regions in the regenerator: the dense phase and the dilute phase (freeboard). The dilute phase is the region above the dense phase up to the cyclone inlet and has a substantially lower catalyst concentration. The dense bed has all of the catalyst contained below the established bed level, where almost all reactions occur. The larger catalyst particles are separated from the gas in the dilute phase and fall back to the bed. Any catalyst particles that do not separate in the dilute phase enter into the regenerator cyclones. Catalyst entering the cyclones is separated by centrifugal force with the larger particles being returned to the bed via the cyclone diplegs. Catalyst fines too small to be separated by the cyclones are carried out of the regenerator with the flue gas.

The regenerator has two main functions: it restores catalyst activity and supplies the endothermic heat required to crack the feed in the riser. In the combustion reaction, the carbon on spent catalyst can be converted to either CO or CO_2 and the hydrogen in the coke is converted into steam. CO oxidation may take the form of either homogeneous oxidation in the gas phase or heterogeneous oxidation in the presence of oxidation promoters.[12,19−23]

The entire mathematical model for the regenerator, developed by Arbel et al.,[13] was adopted for the carbon balance, flue gas composition, and heat balance for the regenerator dense and dilute beds except the model for calculating the dense bed height.[21] All of these model equations for regenerator are given in Appendix B.

3.3. Simulation of FCC Unit. A simulator has been developed where the coupled riser reactor and regenerator model equations have been assembled along with solution procedures. These have been computer coded using C programming language and available with the first author. The ordinary differential equations and nonlinear algebraic equations for material and energy balance are solved by using Runge−Kutta fourth order integration scheme and successive substitution methods, respectively. Tables 1−3 provide data on feed composition, operating data, design data, and thermodynamic and other data, which were used for the present simulation studies. The values of kinetic parameters for the regenerator simulation were used from literature.[5,13]

The solution of the model equations starts with initially guessed values of regenerated catalyst temperature (T_{rgn} = 900 K) and coke on regenerated catalyst (C_{rgc} = 0.0025); the product yields are, then, calculated at the outlet of the reactor. Subsequently the temperature of spent catalyst and coke on spent catalyst are calculated. The regenerator simulation followed by dense bed calculations provide the new values of catalyst temperature (T_{cal}) and coke on regenerated catalyst (C_{cal}) which are compared with the initial value of T_{rgn} and C_{rgc}. If T_{cal} and C_{cal} do not match with assumed T_{rgn} and C_{rgc}, then one needs to start the reactor calculation with newly calculated values of T_{rgn} and C_{rgc} by using the successive substitution method. Finally all of the reactor and regenerator equations are solved with a converged value of T_{rgn} and C_{rgc}. The tolerance for the convergence of T_{rgn} and C_{rgc} used are 1 °C and 10^{-4} kg of coke/(kg of catalyst), respectively. The computational time required for simulation of the FCC unit was 1.5−2 min with ∼10000 iterations for successive substitution.

Table 1. Feed Composition and Properties Used in the Simulation

parameter	values			
	case I	case II	case III	case IV
specific gravity at 15 °C	0.8896	0.8896	0.8858	0.8949
distillation, ASTM D-1160				
0 °C	288	268	253	282
5 °C	370	357	358	352
10 °C	386	383	384	372
30 °C	425	417	416	408
50 °C	450	438	445	437
70 °C	483	464	466	475
90 °C	530	505	509	517
95 °C	542	517	519	536
100 °C	546	525	526	555
CCR, wt %	0.15	0.22	0.21	0.38
total sulfur, wt %	0.5	0.45	0.43	0.34
basic nitrogen, ppm	307	299	281	-
total nitrogen, ppm	900	717	672	-
feed composition from ANN model[17]				
paraffins, wt %	17.7	11.8	12.7	17.2
naphthenes, wt %	33.3	36.6	34.0	21.4
aromatics, wt %	49.0	51.6	53.3	61.5

Table 2. Plant Operating Data Used in Simulation

operating parameter	case I	case II	case III	case IV
feed rate, kg/s	49.3	50.2	46.7	47.2
feed preheat temp, K	621.9	621.0	616.0	614.3
reactor outlet temp, K	767.3	767.4	767.3	767.2
catalyst circulation rate, kg/s	225.0	250.8	237.8	211.8
catalyst density, kg/m^3	817.0	831.0	850.0	800.0
regenerator dense phase temp, K	938.0	935.0	935.0	945.0
reactor pressure, kg/cm2	2.3	2.3	2.2	2.3
regenerator pressure, kg/cm2	2.6	2.6	2.6	2.6
air to regenerator temp, K	470	476	455	490
air rate, kmol/s	0.79	0.80	0.75	0.78
hydrogen in coke, wt %	9.2	16.4	14.3	9.5

3.4. Validation of FCC Model with Plant Data. Several sets of test run data and one set of normal operating data were obtained from an operating FCC plant in a refinery for validation of the developed simulator. A commercial ASPEN FCC simulator[24] was also tuned for the plant data by adjusting nondefault parameters such as stripping efficiency (95%), fraction of nonvaporized feed to coke (0.04), fraction of Concarbon to coke (0.48), and mass ratio of H_2 to metals coke (0.12), etc. The performance of the model has been evaluated by comparing the model predicted values of conversion and yields with the plant data as well as calculated values from ASPEN FCC simulator[24] at the riser outlet for four different cases. The feeds for all of the cases were mixtures of different heavy gas oils from different crude mixes resulting in a wide variation in composition.

Case I. The 10-lump model predicted yields were compared with the first set of refinery plant data, and the results were found to be in good agreement as shown in Table 4. Also

dx.doi.org/10.1021/ie5006433 | Ind. Eng. Chem. Res. XXXX, XXX, XXX−XXX

Table 3. Thermodynamic and Other Parameters Used in Simulation

description	test run
$C_{p,c}$, kJ/(kg·K)	1.29[a]
$C_{p,fl}$, kJ/(kg·K)	3.43[a]
$C_{p,fv}$, kJ/(kg·K)	3.39[a]
ΔH_{evp}, kJ/kg	349[a]
C_{p,N_2}, kJ/(kg·K)	29.12
C_{p,O_2}, kJ/(kg·K)	29.44
C_{p,H_2O}, kJ/(kg·K)	41.01
$C_{p,CO}$, kJ/(kg·K)	29.12
C_{p,CO_2}, kJ/(kg·K)	37.14
H_{CO}, kJ/kmol	110640
H_{CO_2}, kJ/kmol	393520
H_{H_2O}, kJ/kmol	240590
X_{pt}	0.10
D_p, m	6.0×10^{-5}
molecular weight of kinetic lumps, kg/kmol	
P_h, N_h, A_h[b]	339
P_l, N_l, A_l[c]	240
gasoline	114
LPG	54
dry gas	30
coke	12
design data	
riser length, m	37
riser diameter, m	0.7
regenerator length, m	15
regenerator diameter, m	5.6

[a]Data from Arbel et al.[13] [b]P_h = heavy paraffins; N_h = heavy naphthenes; A_h = heavy aromatics. [c]P_l = light paraffins; N_l = light naphthenes; A_l = light aromatics.

included in this table are results obtained from ASPEN FCC simulator for the same operating data. The percent deviation between the plant and the present model as well as the plant and ASPEN FCC were calculated. The deviation between the plant and the present model shows the heavy and light fractions deviated about 5%, whereas the other four products, namely, gasoline, LPG, dry gas, and coke, showed a maximum deviation of 7%. Similar deviations are seen for the ASPEN FCC predictions except with smaller magnitude.

Case II. The model was again validated with second test run data from the same FCC unit but with different feed composition and different operating conditions. Table 4 also shows similar comparisons between the plant measured, ASPEN calculated, and the present model calculated values for case II. The comparison shows a good match between the present model and plant test run with deviations less than 4.5% except for the LPG yield (10.9%). The performance of the ASPEN FCC simulator shows higher deviations from plant data deviating by as much as 16.7%.

Case III. A new set of daily operating data from the plant was used to simulate the model. The results on yields and reactor outlet temperature from plant, ASPEN FCC model, and the present model are shown in Table 5. This case also shows a good match between the present model and plant value for all of the components except dry gas. Dry gas content being small (~1.6%), its measured value is likely to be uncertain to a larger extent because of measurement errors. It may be noted that, for this case, the ASPEN FCC model performance is quite inferior as compared to the present model.

Case IV. The model was finally simulated with yet another set of plant data to facilitate wider comparison between the model calculated values and the plant data, and the results are also shown in Table 5. The matches were found to be in the range of acceptable limits.

From the preceding study with four different sets of real plant data obtained with different feed compositions it can be seen that the present model represents the FCC riser reactor reasonably well. The predictions from the present model are as good as those from ASPEN FCC simulator and at times, even better.

4. FIVE-LUMP KINETIC MODEL

The literature available 5-lump kinetic model[5,7] was reconstructed by determining the new rate constants. It uses only one lump to characterize the feed and hence does not require any ANN prediction. An average molecular weight and an average molecular formula of the type CnHm are assigned to the feed lump which describes the feed. The data that were

Table 4. Comparison of Model Calculated Values with Plant Data (Cases I and II)

	case I			case II		
		calculated values from simulation			calculated values from simulation	
	measured value	ASPEN FCC (% dev)	present model (% dev)	measured value	ASPEN FCC (% dev)	present model (% dev)
riser outlet temp, K	767.3	767.4 (0.0)	768.0 (−0.1)	767.4	767.5 (0.0)	770.9 (−0.5)
P_h,[a] wt %		0.0	0.0		0.0	0.0
N_h,[b] wt %		0.0	0.1		0.0	0.0
A_h,[c] wt %		14.1	13.6		10.8	12.8
total heavy fraction (343+ °C), wt %	14.5	14.2 (2.1)	13.7 (5.3)	12.9	10.8 (16.8)	12.8 (1.2)
P_l,[d] wt %		2.7	2.3		1.3	1.3
N_l,[e] wt %		3.3	2.6		1.5	2.2
A_l,[f] wt %		11.6	11.4		13.7	11.7
total light fraction (221−343 °C), wt %	17.2	17.6 (−2.6)	16.3 (5.2)	15.6	16.4 (−5.2)	15.2 (2.6)
gasoline (C5 − 221 °C), wt %	51.5	50.9 (1.2)	52.1 (−1.2)	54.3	54.8 (−0.9)	53.3 (1.8)
LPG, wt %	11.4	11.8 (−3.4)	12.2 (−6.8)	12.4	12.6 (−1.8)	13.7 (−10.9)
dry gas, wt %	1.5	1.5 (−0.3)	1.7 (−7.4)	1.2	1.6 (−35.1)	1.2 (−3.3)
coke, wt %	4.0	4.1 (−1.6)	4.1 (−3.2)	3.6	3.8 (−6.6)	3.7 (−4.4)

[a]P_h = heavy paraffins. [b]N_h = heavy naphthenes. [c]A_h = heavy aromatics. [d]P_l = light paraffins. [e]N_l = light naphthenes. [f]A_l = light aromatics.

dx.doi.org/10.1021/ie5006433 | Ind. Eng. Chem. Res. XXXX, XXX, XXX−XXX

Table 5. Comparison of Model Calculated Values with Plant Data (Cases III and IV)

	case III			case IV		
		calculated values from simulation			calculated values from simulation	
	measured value	ASPEN FCC (% dev)	present model (% dev)	measured value	ASPEN FCC (% dev)	present model (% dev)
riser outlet temp, K	767.3	767.6 (0.0)	769.7 (−0.3)	767.2	767.4 (0.0)	771 (−0.6)
P_h,[a] wt %		0.0	0.0		0.0	0.0
N_h,[b] wt %		0.0	0.0		0.0	0.1
A_h,[c] wt %		7.8	13.0		15.1	15.4
total heavy fraction (343+ °C), wt %	12.1	7.8 (35.8)	13.0 (−7.4)	14.5	15.1 (−4.4)	15.5 (−7.3)
P_l,[d] wt %		0.4	1.4		1.1	2.4
N_l,[e] wt %		0.6	2.1		1.4	1.9
A_l,[f] wt %		15.1	10.7		17.3	13.3
total light fraction (221−343 °C), wt %	13.9	16.1 (−15.5)	14.2 (−2.2)	20.2	19.7 (2.4)	17.7 (12.7)
gasoline (C5 − 221 °C), wt %	55.8	56.7 (−1.6)	54.1 (3.0)	48.6	48.9 (−0.4)	50.8 (−4.4)
LPG, wt %	12.9	14.2 (−10.3)	13.6 (−5.4)	11.1	11.3 (−1.8)	10.8 (2.8)
dry gas, wt %	1.6	2.0 (−21.9)	1.3 (18.8)	1.4	1.5 (−4.8)	1.4 (−2.7)
coke, wt %	3.7	3.3 (10.5)	3.8 (−2.7)	4.1	3.5 (14.7)	3.8 (8.7)

[a] P_h = heavy paraffins. [b] N_h = heavy naphthenes. [c] A_h = heavy aromatics. [d] P_l = light paraffins. [e] N_l = light naphthenes. [f] A_l = light aromatics.

regressed to obtained kinetic parameters for the 10-lump model were reused to calculate kinetic parameters for the 5-lump model to facilitate comparison between the two models. All of the model equations for the 5-lump kinetic model of FCC riser reactor were adopted from literature[5] and are also available in Appendix A, and recalculated kinetic parameters are given in Table 6. The kinetic parameters were determined for all nine reactions involved in the 5-lump kinetic scheme. The same optimization technique, genetic algorithm[25] (GA) was used to calculate the kinetic parameters as was done in the case of the 10-lump model. The algorithm available in MATLAB Optimization Toolbox was used in the present study.

Table 6. Calculated Kinetic Rate Constants for Five-Lump Model

i[a]	reactions	rate constants
1	gas oil → gasoline	15.4508
2	gas oil → LPG	3.1312
3	gas oil → DG[b]	0.3722
4	gas oil → coke	0.9331
5	gasoline → LPG	0.0035
6	gasoline → DG	0.0003
7	gasoline → coke	0.0016
8	LPG → DG	0.0012
9	LPG → coke	0.0016

[a] i = reaction number. [b] DG = dry gas.

4.1. Comparison of Ten-Lump FCC Kinetic Model with the Five-Lump Kinetic Model. Finally, the results from the 5-lump kinetic model were compared with those from the 10-lump model to establish the following: (1) single lump feed description leads to feed specific rate constants not valid for other feeds; (2) more detailed feed description results in superior prediction capability of the model for a variety of feeds.

Table 7 shows a comparison of model calculated values using both 10-lump and 5-lump kinetics and plant measured experimental values. The 5-lump model was simulated with the literature values[6,7] of rate constants and also using tuned values of rate constants as given in Table 6. While maximum deviation in unconverted gas oil was only 1.9% for the 10-lump model, it was as high as 100% for the 5-lump model when literature values of kinetic parameters were used. The calculated values of products also showed large deviations. These deviations were significantly reduced for the 5-lump model when tuned values of rate constants were used instead of literature values. However, these deviations are still considerably more than those obtained with the 10-lump model. This clearly brings out the strong dependence of rate constants on feed composition and hence the inadequacy of a single-lump description of FCC feed. The fact that predictions made with the 10-lump kinetic description were superior to those using the 5-lump model even after tuning vindicates the validity of the detailed description of the feed used here.

5. PARAMETRIC SENSITIVITY STUDY FOR THE TEN-LUMP MODEL WITH RESPECT TO OPERATING CONDITIONS

It will be interesting to use the previously described FCC simulator to carry out some optimization studies which could be offline or online. A typical offline optimization exercise aims to find operating conditions which optimize an economic or technical objective function subject to all of the model equations and practical bounds on operating conditions as constraints. Online optimization, on the other hand, is a supervisory level control function which may seek to optimize profit over a long time by updating regulatory controller set points from time to time.[26] All of this requires economic and other data which most refineries do not like to share with outsiders. However, plant personnel can use the present simulator for optimization of their FCC units as long as they are processing heavy gas oil as feed. In the absence of requisite economic data, we have carried out parametric sensitivity studies with respect to operating conditions, which may be looked upon as a substitute for offline optimization since it provides the effect of change in each operating condition on the performance of the FCC unit. The feed preheat temperature (T_{feed}), feed flow rate (F_{feed}), and reactor outlet temperature (ROT) are the independent input parameters which were found to influence the FCC operation

dx.doi.org/10.1021/ie5006433 | Ind. Eng. Chem. Res. XXXX, XXX, XXX−XXX

Table 7. Comparison of Ten-Lump and Five-Lump Model Calculated Values with Plant Data (Case II)

		model calculated value		
			5 lump (% dev)	
	measured value	10 lump (% dev)	lit.[a]	tuned[b]
riser outlet temp, K	767.4	770.9 (−0.5)	778.4 (−1.4)	769.5 (−0.3)
P_h[c]		0.0		
N_h[d]		0.0		
A_h[e]		12.8		
total heavy fraction (343+ °C)	12.9	12.8 (1.2)		
P_l[f]		1.3		
N_l[g]		2.2		
A_l[h]		11.7		
total light fraction (221−343 °C)	15.6	15.2 (2.6)		
total unconverted gas oil (221+ °C)	28.5	28.0 (1.9)	57.3 (−100.6)	31.5 (−9.4)
gasoline (C5 − 221 °C)	54.3	53.3 (1.8)	27.2 (49.9)	51.5 (5.6)
LPG	12.4	13.7 (−10.8)	9.8 (21.1)	11.8 (4.7)
dry gas	1.2	1.2 (−3.3)	2.7 (−130.5)	1.5 (−19.1)
coke	3.6	3.7 (−4.4)	3.1 (14.0)	3.8 (−5.2)

[a]Literature kinetic constants[5] used for simulation. [b]Estimated rate constants (from Table 6) used for simulation. [c]P_h = heavy paraffins. [d]N_h = heavy naphthenes. [e]A_h = heavy aromatics. [f]P_l = light paraffins. [g]N_l = light naphthenes. [h]A_l = light aromatics.

most. These independent variables were varied one at a time, keeping the other two constant at their base values and their effect on steady T_{rgn}, air flow rate (F_{air}) into the regenerator for coke combustion, and catalyst circulation rate (CCR) through the riser reactor. Out of these three, two were allowed to vary to keep two of the independent variables constant and the third dependent variable, T_{rgn} or F_{air}, was held constant. Catalyst circulation rate was always allowed to be manipulated due to practical considerations. Another dependent variable which is important is coke on regenerated catalyst (C_{rgc}), but one always wishes to keep it constant at a low value, since an increase in C_{rgc} adversely affects conversion.

5.1. Effect of Variation in T_{feed} Keeping F_{feed} and ROT Constant at Base Value. Two variants were investigated, keeping T_{rgn} constant at one time and F_{air} constant at another time. At constant regenerator temperature, as feed preheat temperature is increased, catalyst circulation rate must decrease to keep ROT constant. At constant feed rate, a decrease in CCR leads to a decrease in conversion as well as product yields as shown in Figure 3. The slopes in this figure are gentler and perhaps more accurate than those reported earlier[8] obtained with the 5-lump model. Figure 4 shows variation in the air flow rate and catalyst circulation rate as T_{feed} increases. As seen in this figure, both F_{air} and CCR decrease continuously and almost linearly but with different slopes. On the other hand, when F_{air} is held constant and T_{rgn} is varied, then while conversion and product yields have the same decreasing trend as seen in Figure 3 but unlike F_{air}, T_{rgn} increases and CCR decreases with an increase in feed temperature. The plots for this case have been omitted for brevity.

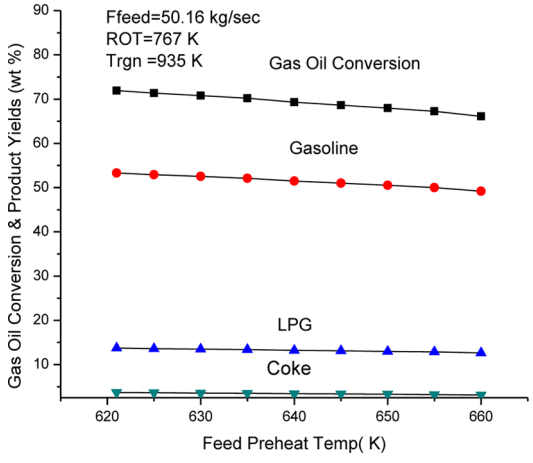

Figure 3. Effect of feed preheat temperature (T_{feed}) on gas oil conversion and product yields at fixed F_{feed} (50.16 kg/s), fixed ROT (767 K), and fixed T_{rgn} (935 K).

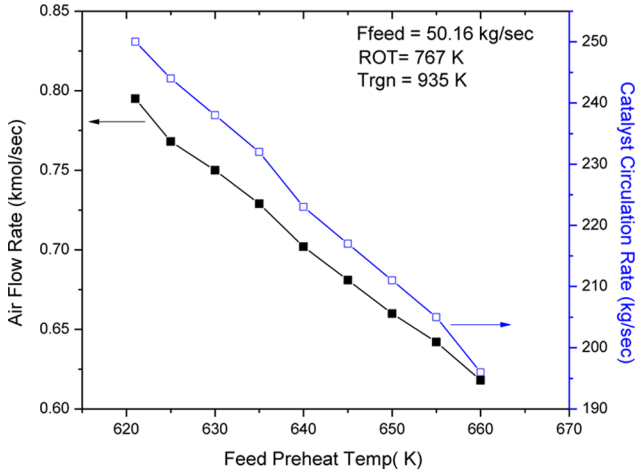

Figure 4. Variation in air flow rate and catalyst circulation rate on increasing feed preheat temp (T_{feed}) at constant T_{rgn} (935 K).

5.2. Effect of Variation in ROT Keeping T_{feed} and F_{feed} Constant at Base Value. As the reactor outlet temperature is increased, the gas oil conversion and product yields increase at constant F_{feed}, T_{feed}, and T_{rgn} (see Figure 5). This is due to an increase in the catalyst circulation rate which leads to more cracking and hence higher yields. Both air flow rate and catalyst circulation rate increase with an increase in ROT at constant T_{rgn} as shown in Figure 6. At higher conversion, coke on the catalyst increases, and to burn this extra coke, the air flow rate has to increase. Constant T_{rgn} keeps coke on regenerated catalyst, C_{rgc}, constant. When F_{air} is held constant at its base value, the regenerator temperature reduces because of less

dx.doi.org/10.1021/ie5006433 | Ind. Eng. Chem. Res. XXXX, XXX, XXX−XXX

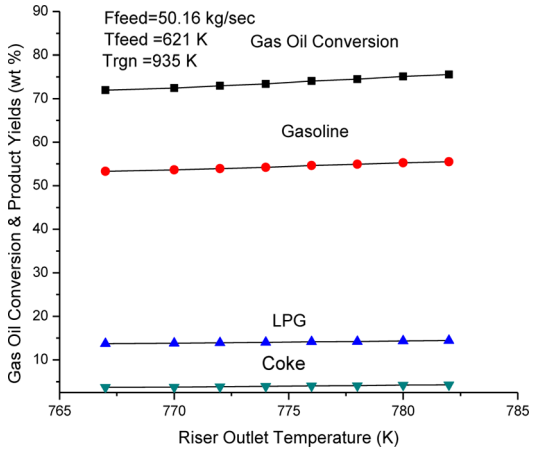

Figure 5. Effect of riser outlet temperature (ROT) on gas oil conversion and product yields at fixed F_{feed} (50.16 kg/s), fixed T_{feed} (621 K), and constant T_{rgn} (935 K).

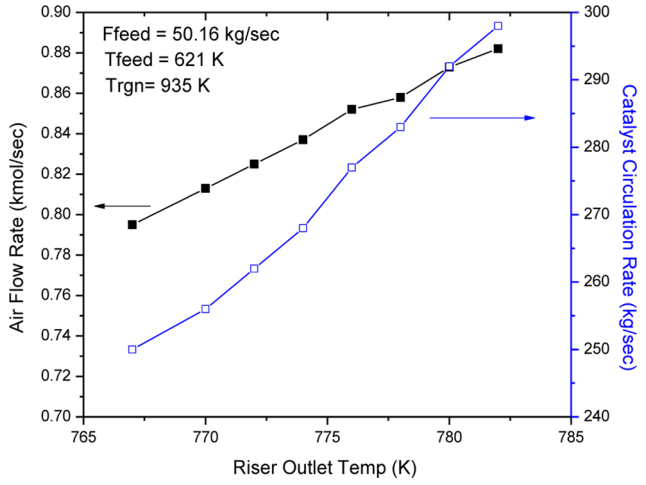

Figure 6. Variation in air flow rate and catalyst circulation rate on increasing ROT at constant T_{rgn} (935 K).

residence time for coke combustion in the regenerator due to an increase in CCR. A decrease in T_{rgn} may lead to an increase in C_{rgc} which is undesirable. However, the effect of increasing catalyst circulation rate is more dominant than the increased value of C_{rgc} when ROT is increased, leading to higher conversion and product yields similar to those seen in Figure 5.

5.3. Effect of Variation in F_{feed} Keeping T_{feed} and ROT Constant at the Base Value. Here again two cases were examined; in one case, T_{rgn} was held constant, and in the other case, F_{air} was fixed. When feed rate increases with T_{rgn} being held constant, the gas oil conversion and product yields marginally decrease similar to that shown in Figure 3. On the regenerator side the air flow rate increases with increased value of feed rate to keep the T_{rgn} constant which keeps C_{rgc} constant. The catalyst circulation rate also increases but slowly. At constant air flow rate, the catalyst circulation rate must increase to keep ROT constant. However, regenerator temperature decreases because of the extra amount of carbon coming in due to higher catalyst circulation with no extra air. This leads to less residence time for burning all of the coke in the regenerator.

6. CONCLUSION

An indigenously developed (and reported[15] earlier) 10-lump kinetic model for the riser reactor was integrated with a regenerator model for the simulation of the entire FCC unit. Several sets of test run data and one set of normal operating data were obtained from an operating FCC plant in a refinery for validation of the developed simulator. The 10-lump model predictions for all of the cases investigated were in close agreement with plant measured values, and deviations were found to be similar to those with ASPEN FCC simulator.

A comparison was made for the present simulator performance with that using 5-lump kinetics for a riser reactor. Significantly larger deviations from measured values were obtained in the case of the 5-lump model as compared to the present simulator, thus establishing the superiority of the model with more detailed description of the feed as compared to the single-lump representation used in the 5-lump model.

Parametric sensitivity study with respect to operating conditions such as the effect of feed preheat temperature, feed flow rate, and reactor outlet temperature showed that the catalyst circulation rate of the riser reactor had stronger influence on gas oil conversion as compared to the feed preheat temperature for a fixed reactor outlet temperature. The sensitivity analysis is useful for the refiners to understand the effects of individual parameters on the FCC performance and to perform an optimization study for better productivity of the unit. From the present sensitivity study, it may be concluded that increasing ROT at fixed T_{rgn} or at fixed F_{air} should lead to improved conversion whereas an increase in F_{feed} or T_{feed} will deteriorate reactor performance. Although the trends observed in this study are similar to those reported earlier,[8] we believe the present results are quantitatively superior and more representative because of improved performance of the 10-lump model.

APPENDIX A. RISER REACTOR MODEL EQUATIONS

A.1. Ten-Lump Model

Material Balance. The mass balance for the jth lump over a differential element of riser height (dh) can be written as follows:

$$\frac{dF_j}{dh} = A_{ris}H_{ris}(1-\varepsilon)\rho_c \sum_{i=1}^{25} (\alpha_{kj})_i r_i;$$

$$i = 1, \ldots, 25 \quad \text{and} \quad j, k = 1, \ldots, 10, \quad j \neq k \qquad \text{(A1)}$$

where

$$(\alpha_{kj})_i = \frac{MW_k}{MW_j} \qquad \text{for } k \rightarrow j \text{ in the } i\text{th reaction}$$

$$h = \frac{Z}{H_{ris}} \qquad \text{(A2)}$$

$$\rho_v = \frac{P_{ris}MW_g}{RT} \quad \text{and} \quad \varepsilon = \frac{F_{feed}/\rho_v}{F_{feed}/\rho_v + F_{rgc}/\rho_c} \qquad \text{(A3)}$$

$$MW_g = \sum_{j=1}^{10} x_j MW_j \qquad \text{(A4)}$$

The rate equation for each ith reaction is as follows:

$$r_i = k_{0,i} \exp\left(-\frac{E_i}{RT}\right) C_j \phi \qquad \text{for } i = 1, 2, 3, 4, 5 \text{ and } j = 1 \qquad \text{(A5)}$$

dx.doi.org/10.1021/ie5006433 | Ind. Eng. Chem. Res. XXXX, XXX, XXX−XXX

$$r_i = k_{0,i}\exp\left(-\frac{E_i}{RT}\right)C_j\phi \quad \text{for } i = 6, 7, 8, 9 \text{ and } j = 2 \tag{A6}$$

$$r_i = k_{0,i}\exp\left(-\frac{E_i}{RT}\right)C_j\phi \quad \text{for } i = 10, 11, 12, 13 \text{ and } j = 3 \tag{A7}$$

$$r_i = k_{0,i}\exp\left(-\frac{E_i}{RT}\right)C_j\phi \quad \text{for } i = 14, 15, 16 \text{ and } j = 4 \tag{A8}$$

$$r_i = k_{0,i}\exp\left(-\frac{E_i}{RT}\right)C_j\phi \quad \text{for } i = 17, 18, 19 \text{ and } j = 5 \tag{A9}$$

$$r_i = k_{0,i}\exp\left(-\frac{E_i}{RT}\right)C_j\phi \quad \text{for } i = 20, 21, 22 \text{ and } j = 6 \tag{A10}$$

$$r_i = k_{0,i}\exp\left(-\frac{E_i}{RT}\right)C_j\phi \quad \text{for } i = 23, 24 \text{ and } j = 7 \tag{A11}$$

$$r_i = k_{0,i}\exp\left(-\frac{E_i}{RT}\right)C_j\phi \quad \text{for } i = 25 \text{ and } j = 8 \tag{A12}$$

The catalyst activity (ϕ) was related to coke concentration on the catalyst[17,18] (C_c):

$$\phi = (1 + 51C_c)^{-2.78} \tag{A13}$$

$$C_c = m\theta^n \tag{A14}$$

The value of m was tuned for the catalyst used from plant data in the present study, whereas the value of the exponent[19] of θ is 0.5.

Energy Balance.

$$\frac{dT}{dh} = \frac{A_{ris}H_{ris}\rho_c(1-\varepsilon)}{F_{rgc}C_{p,c} + F_{feed}C_{p,fv}}\sum_{i=1}^{25} r_i(-\Delta H_i); \quad i = 1, \ldots, 25 \tag{A15}$$

$$T(h{=}0) = \frac{F_{rgc}C_{p,c}T_{rgn} + F_{feed}C_{p,fl}T_{feed} - \Delta H_{evp}F_{feed} - Q_{loss,ris}}{F_{rgc}C_{p,c} + F_{feed}C_{p,fv}} \tag{A16}$$

$Q_{loss,ris}$ in the riser has been taken to be 0.9% of total heat. It can be estimated by trial and error method to match the ROT.

A.2. Five-Lump Riser Reactor Model Equations

Mass Balance.

$$\frac{dF_j}{dh} = A_{ris}H_{ris}(1-\varepsilon)\rho_c\sum_{i=1}^{9}(\alpha_{kj})_i r_i \tag{A17}$$

Rate equations for each of the nine reactions:

$$r_i = k_{0,i}\exp\left(-\frac{E_i}{RT}\right)C_j^2\phi \quad \text{for } i = 1, 2, 3, 4 \text{ and } j = 1 \tag{A18}$$

$$r_i = k_{0,i}\exp\left(-\frac{E_i}{RT}\right)C_j\phi \quad \text{for } i = 5, 6, 7 \text{ and } j = 2 \tag{A19}$$

$$r_i = k_{0,i}\exp\left(-\frac{E_i}{RT}\right)C_j\phi \quad \text{for } i = 8, 9 \text{ and } j = 3 \tag{A20}$$

Enthalpy Balance.

$$\frac{dT}{dh} = \frac{A_{ris}H_{ris}\rho_c(1-\varepsilon)}{F_{rgc}C_{p,c} + F_{feed}C_{p,fv}}\sum_{i=1}^{9} r_i(-\Delta H_i) \tag{A21}$$

$$T(h{=}0) = \frac{F_{rgc}C_{p,c}T_{rgn} + F_{feed}C_{p,fl}T_{feed} - \Delta H_{evp}F_{feed} - Q_{loss,ris}}{F_{rgc}C_{p,c} + F_{feed}C_{p,fv}} \tag{A22}$$

$$MW_g = \sum_{j=1}^{5} x_j MW_j \tag{A23}$$

$$\rho_v = \frac{P_{ris}MW_g}{RT} \quad \text{and} \quad \varepsilon = \frac{F_{feed}/\rho_v}{F_{feed}/\rho_v + F_{rgc}/\rho_c} \tag{A24}$$

A.3. Stripper Modeling

$$T_{sc} = ROT - \Delta T_{sc} \tag{A25}$$

$$F_{sc} = F_{rgc}(1 + C_{sc}) \tag{A26}$$

APPENDIX B. REGENERATOR MODEL EQUATIONS

Main Combustion Reactions in the Regenerator.

$$C + \frac{1}{2}O_2 \xrightarrow{k_{11}} CO$$

$$C + O_2 \xrightarrow{k_{12}} CO_2$$

heterogeneous CO combustion:

$$CO + \frac{1}{2}O_2 \xrightarrow{k_{13,het}} CO_2$$

homogeneous CO combustion:

$$CO + \frac{1}{2}O_2 \xrightarrow{k_{13,hom}} CO_2$$

$$H_2 + \frac{1}{2}O_2 \xrightarrow{k_{14}} H_2O$$

Rate Equations for the Combustion Reactions in the Regenerator.

$$r_{11} = (1-\varepsilon)\rho_c k_{11}\frac{C_{rgc}}{MW_{coke}}P_{O_2} = (1-\varepsilon)\rho_c k_{11}\frac{C_{rgc}}{MW_{coke}}\frac{f_{O_2}}{f_{tot}}P_{rgn} \tag{B1}$$

$$r_{12} = (1-\varepsilon)\rho_c k_{12}\frac{C_{rgc}}{MW_{coke}}P_{O_2} = (1-\varepsilon)\rho_c k_{12}\frac{C_{rgc}}{MW_{coke}}\frac{f_{O_2}}{f_{tot}}P_{rgn} \tag{B2}$$

$$r_{13} = k_{13}P_{O_2}P_{CO} = (X_{pt}(1-\varepsilon)\rho_c k_{13,het} + \varepsilon k_{13,hom})P_{O_2}P_{CO} = (X_{pt}(1-\varepsilon)\rho_c k_{13,het} + \varepsilon k_{13,hom})\frac{f_{O_2}f_{CO}}{f_{tot}}{P_{rgn}}^2 \tag{B3}$$

$$\left(\frac{CO}{CO_2}\right)_{surface} = \frac{k_{11}}{k_{12}} = \beta = \beta_0\exp\left(\frac{-E_\beta}{RT}\right) \tag{B4}$$

$$k_{coke} = k_{11} + k_{12} = k_{coke,0}\exp\left(-\frac{E_{coke}}{RT}\right) \tag{B5}$$

dx.doi.org/10.1021/ie5006433 | Ind. Eng. Chem. Res. XXXX, XXX, XXX−XXX

$$k_{11} = \frac{\beta k_{coke}}{\beta + 1} = \frac{\beta k_{coke,0} \exp\left(-\frac{E_{coke}}{RT}\right)}{\beta + 1} \quad \text{(B6)}$$

$$k_{12} = \frac{k_{coke}}{\beta + 1} = \frac{k_{coke,0} \exp\left(-\frac{E_{coke}}{RT}\right)}{\beta + 1} \quad \text{(B7)}$$

$$k_{13,het} = k_{13,het,0} \exp\left(-\frac{E_{13,het}}{RT}\right) \quad \text{(B8)}$$

$$k_{13,hom} = k_{13,hom,0} \exp\left(-\frac{E_{13,hom}}{RT}\right) \quad \text{(B9)}$$

B.1. Dense Bed Regenerator

Material Balance.

$$\frac{df_{O_2}}{dz} = -A_{rgn}\left(\frac{r_{11}}{2} + r_{12} + \frac{r_{13}}{2}\right) \quad \text{(B10)}$$

$$\frac{df_{CO}}{dz} = -A_{rgn}(r_{13} - r_{11}) \quad \text{(B11)}$$

$$\frac{df_{CO_2}}{dz} = A_{rgn}(r_{12} + r_{13}) \quad \text{(B12)}$$

$$\frac{df_{N_2}}{dz} = 0 \quad \text{(B13)}$$

Initial conditions (at $z = 0$) for dense bed modeling are given as follows:

$$f_{H_2O} = F_{rgc}(C_{sc} - C_{rgc})\frac{C_H}{MW_H} \quad \text{(B14)}$$

$$f_{O_2} = 0.21F_{air} - \frac{1}{2}f_{H_2O} \quad \text{(B15)}$$

$$f_{CO} = f_{CO_2} = 0 \quad \text{(B16)}$$

$$f_{N_2} = 0.79F_{air} \quad \text{(B17)}$$

$$f_{tot} = f_{O_2} + f_{CO} + f_{CO_2} + f_{H_2O} + f_{N_2} \quad \text{(B18)}$$

Energy Balance.

$$\frac{dT_{rgn}}{dz} = 0 \quad \text{(B19)}$$

Heat balance across the regenerator dense bed is given by the following equation:

$$Q_C + Q_H + Q_{air} + Q_{sc} + Q_{ent} = Q_{rgc} + Q_{sg} + Q_{loss} \quad \text{(B20)}$$

where

$$Q_C = f_{CO(Z_{bed})}H_{CO} + f_{CO_2(Z_{bed})}H_{CO_2} \quad \text{(B20a)}$$

$$Q_H = f_{H_2O}H_{H_2O} \quad \text{(B20b)}$$

$$Q_{air} = F_{air}C_{p,air}(T_{air} - T_{base}) \quad \text{(B20c)}$$

$$Q_{sc} = F_{sc}C_{p,sc}(T_{sc} - T_{base}) \quad \text{(B20d)}$$

$$Q_{rgc} = F_{rgc}C_{p,c}(T_{rgn} - T_{base}) \quad \text{(B20e)}$$

$$Q_{sg} = f_{CO_2(Z_{bed})}C_{p,CO_2} + f_{CO(Z_{bed})}C_{p,CO} + f_{O_2(Z_{bed})}C_{p,O_2} + f_{H_2O}C_{p,H_2O} + f_{N_2}C_{p,N_2})(T_{rgn} - T_{base}) \quad \text{(B20f)}$$

$$Q_{ent} = F_{ent}C_{p,c}(T_{dilute(Z_{bed})} - T_{base}) = 0 \quad \text{(assumed)} \quad \text{(B20g)}$$

The final equation for the dense bed temperature is

$$T_{rgn} = T_{base} + \{[f_{CO(Z_{bed})}H_{CO} + f_{CO_2}H_{CO_2} + f_{H_2O}H_{H_2O} + F_{air}C_{p,air}(T_{air} - T_{base}) + F_{sc}C_{p,c}(T_{sc} - T_{base}) + Q_{loss,rgn}] / [F_{rgc}C_{p,c} + f_{CO_2(Z_{bed})}C_{p,CO_2} + f_{CO(Z_{bed})}C_{p,CO} + f_{O_2}C_{p,O_2} + f_{H_2O}C_{p,H_2O} + f_{N_2}C_{p,N_2}]\} \quad \text{(B21)}$$

$$F_{sc}C_{sc}(1 - C_H) = F_{rgc}C_{rgc}(1 - C_H) + (f_{CO(Z_{bed})} + f_{CO_2(Z_{bed})})MW_{coke} \quad \text{(B22)}$$

$$C_{rgc} = [F_{sc}C_{sc}(1 - C_H) - (f_{CO(Z_{bed})} + f_{CO_2(Z_{bed})})MW_{coke}]/[F_{rgc}(1 - C_H)] \quad \text{(B23)}$$

(a) Evaluation of Bed Characteristics.[22,23]

$$\rho_g = \frac{P_{rgn}}{RT_{rgn}} \quad \text{(B24)}$$

$$u = \frac{F_{air}}{\rho_g A_{rgn}} \quad \text{(B25)}$$

$$\varepsilon_{dense} = \frac{0.305u_1 + 1}{0.305u_1 + 2} \quad \text{(B26)}$$

$$\rho_{c,dense} = \rho_c(1 - \varepsilon_{dense}) \quad \text{(B27)}$$

$$\rho_{c,dilute} = \max[0, (0.582u_1 - 0.878)] \quad \text{in (lb/ft}^3\text{)} \quad \text{(B28)}$$

$$\varepsilon_{dilute} = \frac{\rho_{dilute}}{\rho_c} \quad \text{(B29)}$$

$$F_{ent} = \rho_{c,dilute}A_{rgn}u \quad \text{(B30)}$$

(b) Dense Bed Height. The regenerator dense bed height is calculated by the given correlation:[22]

$$Z_{bed} = 0.3048(TDH) \quad \text{(B31)}$$

where

$$TDH = TDH_{20} + (D - 20)$$

$$\log(TDH_{20}) = \log(20.5) + 0.07(u_1 - 3)$$

B.2. Dilute Bed Regenerator

Material Balance.

$$\frac{df_{O_2}}{dz} = -A_{rgn}\left(\frac{r_{11}}{2} + r_{12} + \frac{r_{13}}{2}\right) \quad \text{(B32)}$$

$$\frac{df_{CO}}{dz} = -A_{rgn}(r_{13} - r_{11}) \quad \text{(B33)}$$

$$\frac{df_{CO_2}}{dz} = A_{rgn}(r_{12} + r_{13}) \quad \text{(B34)}$$

dx.doi.org/10.1021/ie5006433 | Ind. Eng. Chem. Res. XXXX, XXX, XXX−XXX

$$\frac{df_C}{dz} = -A_{rgn}(r_{11} + r_{12}) \quad \text{(B35)}$$

Energy Balance.p

$$\frac{dT_{dilute}}{dz} = \frac{1}{C_{p,tot}}\left(H_{CO}\frac{df_{CO}}{dz} + H_{CO_2}\frac{df_{CO_2}}{dz}\right) = \frac{A_{rgn}}{C_{p,tot}f_{tot}}[H_{CO}(r_{11} - r_{12}) + H_{CO_2}(r_{11} - r_{12})] \quad \text{(B36)}$$

where

$$C_{p,tot} = (C_{p,N_2}f_{N_2} + C_{p,O_2}f_{O_2} + C_{p,CO}f_{CO} + C_{p,CO_2}f_{CO_2} + C_{p,H_2O}f_{H_2O} + C_{p,c}F_{ent})/f_{tot}$$

Nomenclature

A_{rgn}	regenerator cross-section area, m^2
A_{ris}	riser cross-sectional area, m^2
C_c	coke on catalyst, kg of coke/(kg of catalyst)
C_H	weight fraction of hydrogen in coke, (kg of H_2)/(kg of coke)
C_j	concentration of jth component, kmol/m^3
$C_{p,c}$	catalyst heat capacity, kJ/(kg·K)
$C_{p,CO}$	mean heat capacity of CO, kJ/(kg·K)
C_{p,CO_2}	mean heat capacity of CO_2, kJ/(kg·K)
$C_{p,fl}$	liquid feed heat capacity, kJ/(kg·K)
$C_{p,fv}$	vapor feed heat capacity, kJ/(kg·K)
C_{p,H_2O}	mean heat capacity of water, kJ/(kg·K)
C_{p,N_2}	mean heat capacity of N_2, kJ/(kg·K)
C_{p,O_2}	mean heat capacity of O_2, kJ/(kg·K)
C_{rgc}	coke on regenerator catalyst, (kg of coke)/(kg of catalyst)
C_{sc}	coke on spent catalyst, (kg of coke)/(kg of catalyst)
D	regenerator diameter, ft
E_β	activation energy for CO/CO_2 at the catalyst surface
E_i	activation energy of ith cracking reaction in the riser
E_{coke}	activation energy of coke combustion
$E_{13,het}$	activation energy for heterogeneous CO combustion
$E_{13,hom}$	activation energy for homogeneous CO combustion
f_C	molar flow rate of carbon in the regenerator, kmol/s
f_{CO}	CO molar flow rate in the regenerator, kmol/s
f_{CO_2}	CO_2 molar flow rate in the regenerator, kmol/s
f_{H_2O}	H_2O molar flow rate in the regenerator, kmol/s
f_{N_2}	N_2 molar flow rate in the regenerator, kmol/s
f_{O_2}	O_2 molar flow rate in the regenerator, kmol/s
f_{tot}	total gas molar flow rate in the regenerator, kmol/s
F_{air}	air flow rate to the regenerator, kmol/s
F_{ent}	entrained catalyst flow rate kg/s
F_{feed}	oil feed flow rate, kg/s
F_j	molar flow rate of jth lump, kmol/s
F_{rgc}	catalyst circulation rate (CCR), kg/s
F_{sc}	spent catalyst flow rate, kg/s
h	dimensionless riser height
H_{CO}	heat of formation of oil feed, kJ/kmol
H_{CO_2}	heat of formation of CO_2, kJ/kmol
H_{H_2O}	heat of formation of H_2O, kJ/kmol
H_{ris}	riser height, m
ΔH_{evp}	heat of vaporization of oil feed, kJ/kg
ΔH_i	heat of cracking of ith lump, kJ/kmol
i	total no. of reactions in the reactor
j	total no. of kinetic lumps
k_i	rate constant of ith reaction in the riser, m^3/((kg of catalyst)·s)
$k_{0,i}$	frequency factor for ith reaction in the riser, m^3/((kg of catalyst)·s)
k_{11}	coke combustion rate coefficient for C to CO reaction
k_{12}	coke combustion rate coefficient for C to CO_2 reaction
k_{coke}	total coke combustion rate coefficient, 1/(atm·s)
$k_{coke,0}$	frequency factor for coke combustion, 1/(atm·s)
$k_{13,het}$	frequency factor in heterogeneous CO combustion expression, (kmol of CO)/((kg of catalyst)·m^3·s)
$k_{13,hom}$	frequency factor in homogeneous CO combustion expression, (kmol of CO)/(m^3·atm^2·s)
MW_j	molecular weight of jth lump, kg/kmol
MW_{coke}	molecular weight of coke, kg/kmol
MW_g	average molecular weight of gas oil feed, kg/kmol
MW_H	molecular weight of hydrogen
P_{ris}	riser pressure, atm
P_{rgn}	regenerator pressure, atm
P_{O_2}	average mean oxygen partial pressure, atm
Q_{air}	heat flow rate with air, kJ/s
Q_C	heat released by the carbon combustion, kJ/s
Q_{ent}	heat input to the dense bed from entrained catalyst returning from cyclone, kJ/s
Q_H	heat released by the hydrogen combustion, kJ/s
$Q_{loss,rgn}$	heat losses from the regenerator, kJ/s
$Q_{loss,ris}$	heat losses from the riser base, kJ/s
Q_{rgc}	heat flow with regenerated catalyst, kJ/s
Q_{sc}	heat flow rate with spent catalyst, kJ/s
Q_{sg}	heat flow rate with gases from the regenerator dense bed, kJ/s
R	universal gas constant
r_i	rate of the ith reaction, kmol/((kg of catalyst)·s)
ROT	riser outlet temperature, K
T	riser temperature at any axial height, K
T_{air}	temperature of the air to the regenerator
T_{base}	base temperature for heat balance calculations, K (assumed, 866.6 K)
T_{dilute}	regenerator dilute bed temperature, K
T_{feed}	gas oil feed temperature, K
T_{rgn}	regenerator dense bed temperature/regenerated catalyst temperature, K
T_{sc}	temperature of spent catalyst, K
ΔT_{st}	stripper temperature drop (~10 °C)
u	velocity of gas in the riser or the regenerator, m/s
u_1	superficial linear velocity, ft/s
X_{pt}	relative catalytic CO combustion rate
x_j	mole fraction of jth component
z	axial height from the entrance of the riser or regenerator, m
Z_{bed}	regenerator dense bed height, m
Z_{dilute}	regenerator dilute phase height, m
Z_{rgn}	regenerator height, m

Greek Letters

$(\alpha_{kj})_i$	stoichiometric coefficient for lump $k \rightarrow j$ in ith reaction
β	CO/CO_2 ratio at the surface in the regenerator
β_0	frequency factor in β expression
ε	riser or regenerator void fraction
θ	catalyst residence time, s
ρ_c	catalyst density, kg/m^3
$\rho_{c,dense}$	catalyst density in the regenerator dense bed, kg/m^3
$\rho_{c,dilute}$	catalyst density in the dilute phase of the regenerator, kg/m^3

dx.doi.org/10.1021/ie5006433 | Ind. Eng. Chem. Res. XXXX, XXX, XXX−XXX

ρ_g molar gas density in the regenerator, kmol/m^3
ρ_v oil vapor density, kg/m^3
ϕ catalyst activity

AUTHOR INFORMATION

Corresponding Author

*Tel.: +91-28840-12312. Fax: +91-28840-26329. E-mail: dasila.prabha@gmail.com.

Notes

The authors declare no competing financial interest.

ACKNOWLEDGMENTS

We gratefully acknowledge Indian Oil Corp. Ltd. (IOCL) and University of Petroleum & Energy Studies for allowing us to publish the present work. P.K.D. acknowledges financial support from IOCL.

REFERENCES

(1) Weekman, V. W., Jr. A Model of Catalytic Cracking Conversion in Fixed, Moving, and Fluid Bed Reactors. *Ind. Eng. Chem. Process Des. Dev.* **1968**, *7*, 90.

(2) Weekman, V. W., Jr. Kinetics and Dynamics of Catalytic Cracking Selectivity in Fixed Bed Reactors. *Ind. Eng. Chem. Process Des. Dev.* **1969**, *8*, 385.

(3) Lee, L.; Chen, Y.; Huang, T. Four-Lump Kinetic Model for Fluid Catalytic Cracking Process. *Can. J. Chem. Eng.* **1989**, *67*, 615.

(4) Abul-Hamayel, M. A. Kinetic Modeling of High-Severity Fluidized Catalytic Cracking. *Fuel* **2003**, *82*, 1113.

(5) Dave, D. J.; Saraf, D. N. A Model Suitable for Rating and Optimization of Industrial FCC Units. *Ind. Chem. Eng., Sect. A* **2003**, *45*, 7.

(6) Ancheyta, J. J.; Lopez, I. F.; Aguilar, R. E. 5-Lump Kinetic Model for Gas Oil Catalytic Cracking. *Appl. Catal., A* **1999**, *177*, 227.

(7) Bollas, G. M.; Lappas, A. A.; Iatridis, D. K.; Vasalos, I. A. Five Lump Kinetic Model with Selective Catalyst Deactivation for the Prediction of the Product Selectivity in the Fluid Catalytic Cracking Process. *Catal. Today* **2007**, *127*, 31.

(8) Dasila, P. K.; Choudhury, I.; Saraf, D. N.; Chopra, S.; Dalai, A. Parametric Sensitivity Studies in a Commercial FCC Unit. *Adv. Chem. Eng. Sci.* **2012**, *2*, 136.

(9) Kasat, R. B.; Kunzru, D.; Saraf, D. N.; Gupta, S. K. Multiobjective Optimization of Industrial FCC Units Using Elitist Nondominated Sorting Genetic Algorithm. *Ind. Eng. Chem. Res.* **2002**, *41*, 4765.

(10) Jacob, S. M.; Gross, B.; Voltz, S. E.; Weekman, V. W., Jr. A Lumping and Reaction Scheme for Catalytic Cracking. *AIChE J.* **1976**, *22*, 701.

(11) Gross, B.; Jacob, S. M.; Nace, D. M.; Voltz, S. E. Simulation of Catalytic Cracking Process. U.S. Patent US3960707, 1976.

(12) Kumar, S.; Chadha, A.; Gupta, R.; Sharma, R. CATCRACK: A Process Simulator for an Integrated FCC-Regenerator System. *Ind. Eng. Chem. Res.* **1995**, *34*, 3737.

(13) Arbel, A.; Huang, Z.; Rinard, I. H.; Shinnar, R. Dynamic and Control of Fluidized Catalytic Crackers. 1. Modeling of the Current Generation of FCC's. *Ind. Eng. Chem. Res.* **1995**, *34*, 1228.

(14) Cerqueira, S. H.; Biscaia, E. C., Jr.; Sousa-Aguiar, E. F. Mathematical Modeling and Simulation of Catalytic Cracking of Gas Oil in a Fixed Bed: Coke Formation. *Appl. Catal., A* **1997**, *164*, 35.

(15) Dasila, P. K. Kinetic Modeling and Simulation of Fluid Catalytic Cracking Units. Ph.D Thesis, University of Petroleum and Energy Studies, Dehradun, India, April 2013.

(16) Dasila, P. K.; Choudhury, I. R.; Saraf, D. N.; Kagdiyal, V.; Rajagopal, S.; Chopra, S. J. Estimation of FCC Feed Composition from Routinely Measured Lab Properties through ANN Model. *Fuel Process. Technol.* **2014**, *125*, 155.

(17) Yingxun, S. Deactivation by Coke in Residuum Catalytic Cracking. In *Catalysts Deactivation*; Bartholomew, C. H., Butt, J. B., Eds.; Elsevier: Amsterdam, 1991; Vol *68*, p 327.

(18) Voorhies, A. Carbon Formation in Catalytic Cracking. *Ind. Eng. Chem.* **1945**, *37*, 318.

(19) Avidan, A. A. Origin, Development, and Scope of FCC Catalysis. In *Fluid Catalytic Cracking: Science and Technology: Studies in Surface Science and Catalysis*; Magee, J. S., Mitchell, M. M., Jr., Eds.; Elsevier: Amsterdam, Netherlands, 1993; Vol *76*, pp 1.

(20) Avidan, A. A.; Shinnar, R. Development of Catalytic Cracking Technology. A Lesson in Chemical Reactor Design. *Ind. Eng. Chem. Res.* **1990**, *29*, 931.

(21) Krishna, A. S.; Parkin, E. S. Modeling the Regenerator in Commercial Fluid Catalytic Cracking Units. *Chem. Eng. Prog.* **1985**, *81*, 57.

(22) Ewell, R. B.; Gadmer, G. Design Cat Crackers by Computer. *Hydrocarbon process* **1978**, *4*, 125.

(23) McFarlane, R. C.; Reineman, R. C.; Bartee, J. F.; Georgakis, C. Dynamic Simulation for a Model IV Fluid Catalytic Cracking Unit. *Comput. Chem. Eng.* **1993**, *17*, 275.

(24) Aspen FCC User's Guide. Aspen Technology, Inc.: Burlington, MA. USA, 2006, http://www.aspentech.com.

(25) Balasubramanian, P.; Bettina, S. J.; Pushpavanam, S.; Balaraman, K. S. Kinetic Parameter Estimation in Hydrocracking Using a Combination of Genetic Algorithm and Sequential Quadratic Programming. *Ind. Eng. Chem. Res.* **2003**, *42*, 4723.

(26) Basak, K.; Abhilash, K. S.; Ganguly, S.; Saraf, D. N. Online Optimization of a Crude Distillation Unit with Constraints on Product Properties. *Ind. Eng. Chem. Res.* **2002**, *41*, 1557.